Manual Therapy xxx (2014) 1–7

Contents lists available at ScienceDirect

Manual Therapy

journal homepage: www.elsevier.com/math

Original article

Biomechanical analysis of two-step traction therapy in the lumbar spine

Won Man Park [a], Kyungsoo Kim [b], Yoon Hyuk Kim [a, *]

[a] Department of Mechanical Engineering, Kyung Hee University, Yongin-si, Gyeonggi-do 446-701, Republic of Korea
[b] Department of Applied Mathematics, Kyung Hee University, Yongin-si, Gyeonggi-do 446-701, Republic of Korea

ARTICLE INFO

Article history:
Received 25 November 2013
Received in revised form
9 April 2014
Accepted 9 May 2014
Available online xxx

Keywords:
Lumbar spine
Traction therapy
Finite element analysis
Biomechanics

ABSTRACT

Traction therapy is one of the most common conservative treatments for low back pain. However, the effects of traction therapy on lumbar spine biomechanics are not well known. We investigated biomechanical effects of two-step traction therapy, which consists of global axial traction and local decompression, on the lumbar spine using a validated three-dimensional finite element model of the lumbar spine. One-third of body weight was applied on the center of the L1 vertebra toward the superior direction for the first axial traction. Anterior translation of the L4 vertebra was considered as the second local decompression. The lordosis angle between the superior planes of the L1 vertebra and sacrum was 44.6° at baseline, 35.2° with global axial traction, and 46.4° with local decompression. The fibers of annulus fibrosus in the posterior region, and intertransverse and posterior longitudinal ligaments experienced stress primarily during global axial traction, these stresses decreased during local decompression. A combination of global axial traction and local decompression would be helpful for reducing tensile stress on the fibers of the annulus fibrosus and ligaments, and intradiscal pressure in traction therapy. This study could be used to develop a safer and more effective type of traction therapy.

© 2014 Elsevier Ltd. All rights reserved.

1. Introduction

Low back pain is one of the most common complaints in the general population, affecting about 80% of the population at some point in life (Kelsey and White, 1980; Manchikanti, 2000). Conservative treatments, such as rest, exercise, and anti-inflammatory drugs, are often used to treat spinal pain (Hilibrand and Rand, 1999; Gluck et al., 2008; Majid and Fischgrund, 2008). Traction therapy is one of the most common conservative treatments for low back pain. Traction therapy is proposed to relieve pain and to recover joint functions by reducing pressure on discs or nerves (Harrison et al., 2002a,b; Paulk and Harrison, 2004; Horseman and Morningstar, 2008; Apfel et al., 2010; Gagne and Hasson, 2010; Kurutz and Bender, 2010; Diab and Moustafa, 2012). Even though there is a controversy regarding the efficacy of traction for back pain (Maher, 2004) and a case study in which the occurrence of large disc protrusion during motorized traction therapy was reported (Deen et al., 2003), the clinical reliability of traction therapy has been investigated in a number of studies (Harrison et al., 2002a,b; Paulk and Harrison, 2004; Macario and Pergolizzi, 2006; Daniel, 2007; Kurutz and Bender, 2010; Kurutz and Oroszvary, 2010; Diab and Moustafa, 2012).

A small number of studies has investigated the biomechanical effects of traction. Ramos and Martin (1994) measured changes in intradiscal pressure during axial traction with a motorized traction device. They have reported quantitative reduction in intradiscal pressure using a cannula inserted pressure transducer at L4–L5 disc, and inverse relation between intradiscal pressure and applied tension was shown in the study. Kurutz and Oroszvary (2010) analyzed the biomechanical effects of hydrotraction therapy on the intervertebral discs using finite element (FE) models that incorporated age-related intervertebral disc degeneration. They reported that direct traction deformations are 15–90% of the indirect one, while the direct traction load is 6% of indirect one in hydrotraction therapy consisting indirect and direct traction loads. Nonetheless, relatively little is known about the effects of traction therapy on lumbar spine biomechanics, including the stresses on the fibers of the annulus fibrosus and ligaments and the forces on the facet joints.

The purpose of this study was to investigate the biomechanics of the spine in a two-step traction therapy, which consists of global axial traction and local decompression, using FE analysis. Changes

* Corresponding author. Tel.: +82 31 201 2028; fax: +82 31 202 8106.
E-mail address: yoonhkim@khu.ac.kr (Y.H. Kim).

http://dx.doi.org/10.1016/j.math.2014.05.004
1356-689X/© 2014 Elsevier Ltd. All rights reserved.

Please cite this article in press as: Park WM, et al., Biomechanical analysis of two-step traction therapy in the lumbar spine, Manual Therapy (2014), http://dx.doi.org/10.1016/j.math.2014.05.004

in the lordosis angle, tissue stress on the fibers of the annulus fibrosus, ligaments stress, intradiscal pressure, and facet joint contact forces during two-step traction therapy were determined. Because it is difficult to measure the amount of stress on the fibers of the annulus fibrosus and ligaments that is related to the damage in these soft-tissues, FE analysis was chosen for this biomechanical study.

2. Materials and methods

In order to measure biomechanical behaviors of the lumbar spine, such as lordosis angle, intradiscal pressure, stresses on the fibers of annulus fibrosus and ligaments, and facet joint forces, with traction, a validated three-dimensional FE model of the lumbar spine was used (Park et al., in press). Computed tomographic scans in 1 mm slices were taken from a healthy male volunteer (170 cm, 66 kg). Three-dimensional FE models of the lumbar vertebrae from L1 to the sacrum were reconstructed from the CT scans. Intervertebral discs were modeled between the vertebrae based on a previously developed modeling technique that used hyperelastic solid elements (annulus ground substance), linear elastic solid elements (end plates), tension-only truss elements (fibers of the annulus fibrosus), and fluid elements (nucleus pulposus). The initial intradiscal pressure was set to zero in this study.

Stiffness of the annulus fibers was increased from the center to the outer region and stress–strain curves of the annulus fibers were adapted from literatures (Shirazi-Adl et al., 1986; Schmidt et al., 2006). Cross-sectional areas of annulus fibers were calculated that makes fiber content of 19% of the annulus volume (Natarajan and Andersson, 1999). Seven major ligaments – the anterior longitudinal ligament (ALL), posterior longitudinal ligament (PLL), ligament flavum (LF), interspinous ligament (ISL), supraspinous ligament (SSL), intertransverse ligament (TL), and capsular ligament (CL) – were attached on the basis of anatomical information using tension-only truss elements. Non-linear stiffnesses were used for seven major ligaments (Rohlmann et al., 2006). Articular cartilage was modeled using linear elastic solid elements, and surface-to-surface contact conditions were applied for the facet joints. All material properties of the bones and soft-tissues were adapted from previously published studies (Table 1) (Shirazi-Adl et al., 1986; Ueno and Liu, 1987; Goel et al., 1995; Lu et al., 1996; Natarajan and Andersson, 1999; Natarajan et al., 2000; Wagner and Lotz, 2004; Rohlmann et al., 2006; Schmidt et al., 2006, 2007a,b; 2009; Guan et al., 2007; Park et al., 2009; Ruberte et al., 2009; Kim et al., 2010). Spinal muscles were not included in the developed FE model. In previous computational studies by using FE analysis, developed FE models were validated by comparing intersegmental ranges of motions (ROMs) and/or moment rotation curves (Shirazi-Adl et al., 1986; Ueno and Liu, 1987; Natarajan and Andersson, 1999; Zander et al., 2001; Eberlein et al., 2004; Guan et al., 2006; Rohlmann et al., 2006; Ruberte et al., 2009; Moramarco et al., 2010). The model used in this study also validated on the aspects of moment rotation curves and ROMs at all motion segment units (MSUs) in various loading conditions.

For two-step traction therapy, we determined the interaction between the bed and the patient as 1) the patient was lying on the bed, 2) the patient's hip and trunk were both on the bed during two-step traction therapy due to the patient's body weight (BW) and/or tightening bands, 3) the bed on which the patient's hip was lying was separate from the bed on which the trunk was lying, and 4) two-step traction therapy was symmetric across the mid-sagittal plane. The relative motions of the L1 vertebra and sacrum could be generated with motions of the upper body and lower body, respectively. Thus, all translational movement of the sacrum was constrained in all directions, and translation of the L1 vertebra in the axial direction was allowed for axial traction. In addition, only flexion–extension rotational movements of the L1 vertebra and the sacrum were allowed in order to avoid over-constraint (Fig. 1).

Two-step traction therapy consisted of the following. The first step was global axial traction. An axial traction force of 216 N (which is about one-third of body weight of the volunteer) was applied in the axial direction at the center of the L1 vertebra toward the superior direction. The second step was local decompression. The reverse side of the lower facet joint of the L4 vertebra was pushed during the second step as much as 7.0 mm, which is about 20% of the anterior–posterior length of the vertebral body of the L4 vertebra. Kinematic boundary condition was used generate anterior translation of the L4 vertebra. The axial traction force and translation of the L4 vertebra were applied in 10% increments.

During two-step traction, we investigated the changes in the lordosis angle, intradiscal pressure, stress on the fibers of the annulus fibrosus and ligaments, and facet joint forces for each MSU. The annulus fibrosus was divided into anterior, lateral, and posterior regions, and the change in the average stress in each region was analyzed. The commercial FE analysis software Abaqus Standard v. 6.10 (Simulia, Providence, RI, USA) and pre- and post-processing software FEMap 10.1.1 (MSC.Software Co., Santa Ana, CA, USA) were used for this study.

3. Results

3.1. Lordosis angle

The lordosis angle between the superior planes of the upper and lower vertebrae was measured at each MSU in the sagittal plane during two-step traction therapy (Fig. 2). The initial angles were 5.4°, 5.3°, 9.0°, 8.1°, and 16.6° at the L1–L2, L2–L3, L3–L4, L4–L5, and L5–S1 MSUs, respectively. When 1/3 BW was applied for global axial traction, the angles at the L1–L2, L2–L3, L3–L4, L4–L5, and L5–S1 MSUs decreased to 5.1°, 3.5°, 6.4°, 5.1°, and 15.1°, respectively; these values changed to 5.5°, 5.4°, 9.9°, 9.1°, and 16.4°, respectively, in the second step.

Table 1
Material properties of the FE model of the lumbar spine (Shirazi-Adl et al., 1986; Ueno and Liu, 1987; Goel et al., 1995; Lu et al., 1996; Natarajan and Andersson, 1999; Natarajan et al., 2000; Wagner and Lotz, 2004; Guan et al., 2006; Rohlmann et al., 2006; Schmidt et al., 2006, 2007a,b, 2009; Park et al., 2009; Ruberte et al., 2009; Kim et al., 2010).

Component	Element type	No. of element	Young's modulus E (MPa)	Poisson ratio (ν)
Cortical bone	Solid	67,939	12,000	0.3
Cancelous bone	Solid	14,160	100	0.2
Post bone	Solid	21,261	3,500	0.25
Cartilaginous Endplate	Solid	4,040	23.8	0.4
Articular cartilage	Solid	496	11	0.4
Nucleus pulposus	Fluid	3,190	Compressibility: 0.0005 mm^2/N	
Annulus ground substance	Solid	8,250	Hyperelastic material (Mooney-rivlin; $C_1 = 0.18$, $C_2 = 0.045$)	
Annulus fibrosus	Truss	19,800	Non-linear elastic	
Ligaments	Truss	186	Non-linear elastic	

Please cite this article in press as: Park WM, et al., Biomechanical analysis of two-step traction therapy in the lumbar spine, Manual Therapy (2014), http://dx.doi.org/10.1016/j.math.2014.05.004

ARTICLE IN PRESS

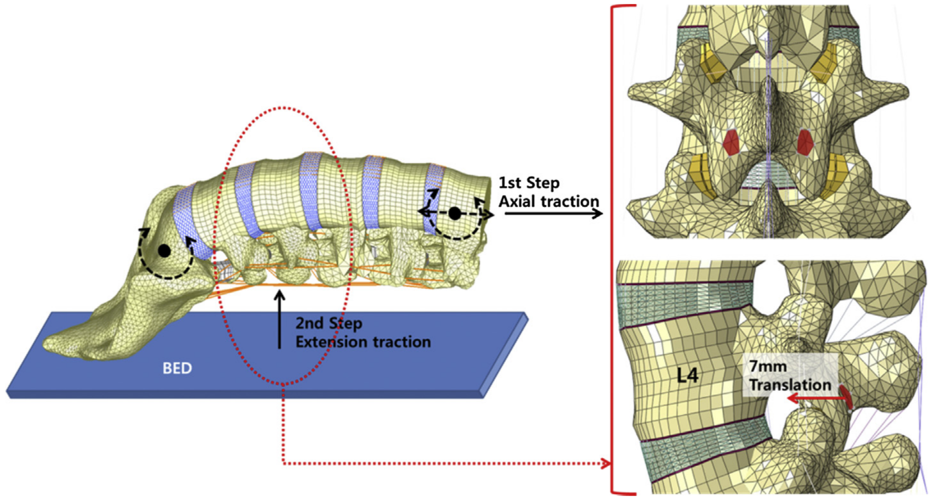

Fig. 1. Boundary and loading conditions for our investigation of the effects of two-step traction therapy on the lumbar spine. The sacrum and L1 vertebra were allowed to rotate in the flexion–extension direction, and the L1 vertebra was allowed to translate in the axial direction.

3.2. *Intradiscal pressure*

The initial intradiscal pressure at each MSU was assumed to be zero in modeling. Thus, the values for intradiscal pressure are only meaningful as relative values. The values for intradiscal pressure decreased by 0.15 MPa, 0.13 MPa, 0.13 MPa, 0.13 MPa, and 0.08 MPa at the L1–L2, L2–L3, L3–L4, L4–L5, and L5–S1 MSUs, respectively, when 1/3 BW was applied for global traction. During the second step of local decompression, intradiscal pressure decreased to −0.18 MPa (at 7.0 mm translation of L4) at the L1–L2 MSU; decreased to −0.15 MPa (at 5.6 mm translation of L4) at the L2–L3 MSU; decreased to −0.15 MPa (at 4.2 mm translation of L4); increased to −0.14 MPa (at 7.0 mm translation of L4) at the L3–L4 MSU; decreased to −0.18 MPa (at 7.0 mm translation of L4) at the L4–L5 MSU; and decreased to −0.15 MPa (at 7.0 mm translation of L4) at the L5–S1 MSU (Fig. 3).

3.3. *Average stresses on the fibers of the annulus fibrosus*

At the L1–L2 MSU, the fibers in the lateral annulus fibrosus showed the highest increase in average stress (0.63 MPa) during the first global traction (Fig. 4). Average stress in the posterior

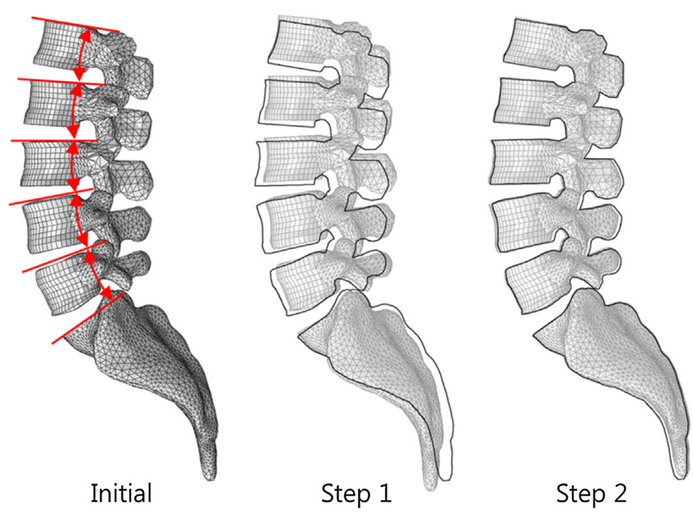

Lordosis angle	Initial	Step 1	Step 2
L1-L2	5.4°	5.1°	5.5°
L2-L3	5.3°	3.5°	5.4°
L3-L4	9.0°	6.4°	9.9°
L4-L5	8.1°	5.1°	9.1°
L5-S1	16.6°	15.1°	16.4°

Fig. 2. Lordosis angles between the superior planes of the upper and lower vertebrae during two-step traction therapy. The solid lines in steps 1 and 2 show the initial locations of the vertebrae.

Please cite this article in press as: Park WM, et al., Biomechanical analysis of two-step traction therapy in the lumbar spine, Manual Therapy (2014), http://dx.doi.org/10.1016/j.math.2014.05.004

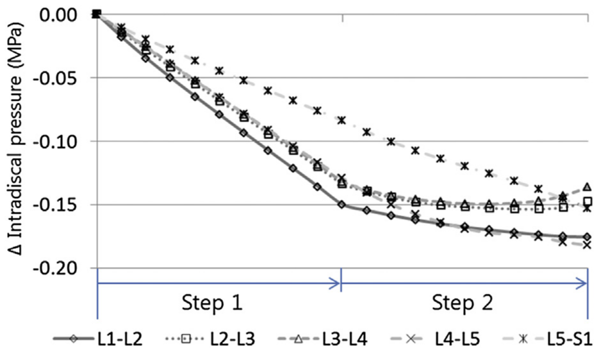

Fig. 3. Changes in intradiscal pressures at L1–L2, L2–L3, L3–L4, L4–L5, and L5–S1 MSUs during two-step traction.

region was as high as 80% of the stress in the lateral region. At the other MSUs, the highest average stresses were shown in the posterior region, and the values at L2–L3, L3–L4, L4–L5 and L5–S1 MSUs were 0.75 MPa, 0.46 MPa, 1.07 MPa, and 1.31 MPa, respectively. The average stress in the posterior region decreased for all MSUs with increments of translation of the L4 vertebra. While the stresses in the lateral regions decreased in the L2–L3, L3–L4, and L4–L5 MSUs during early translation of the L4 vertebra, the stresses increased when the L4 vertebra was translated more than 2.1–4.2 mm.

3.4. Stresses on the ligaments

All ligaments were modeled to act only in tension. Fig. 5 shows changes in the stresses on all ligaments during two-step traction. The ALL was stressed only at the L1–L2 MSU during the first step of global axial traction, and the stress continuously increased during

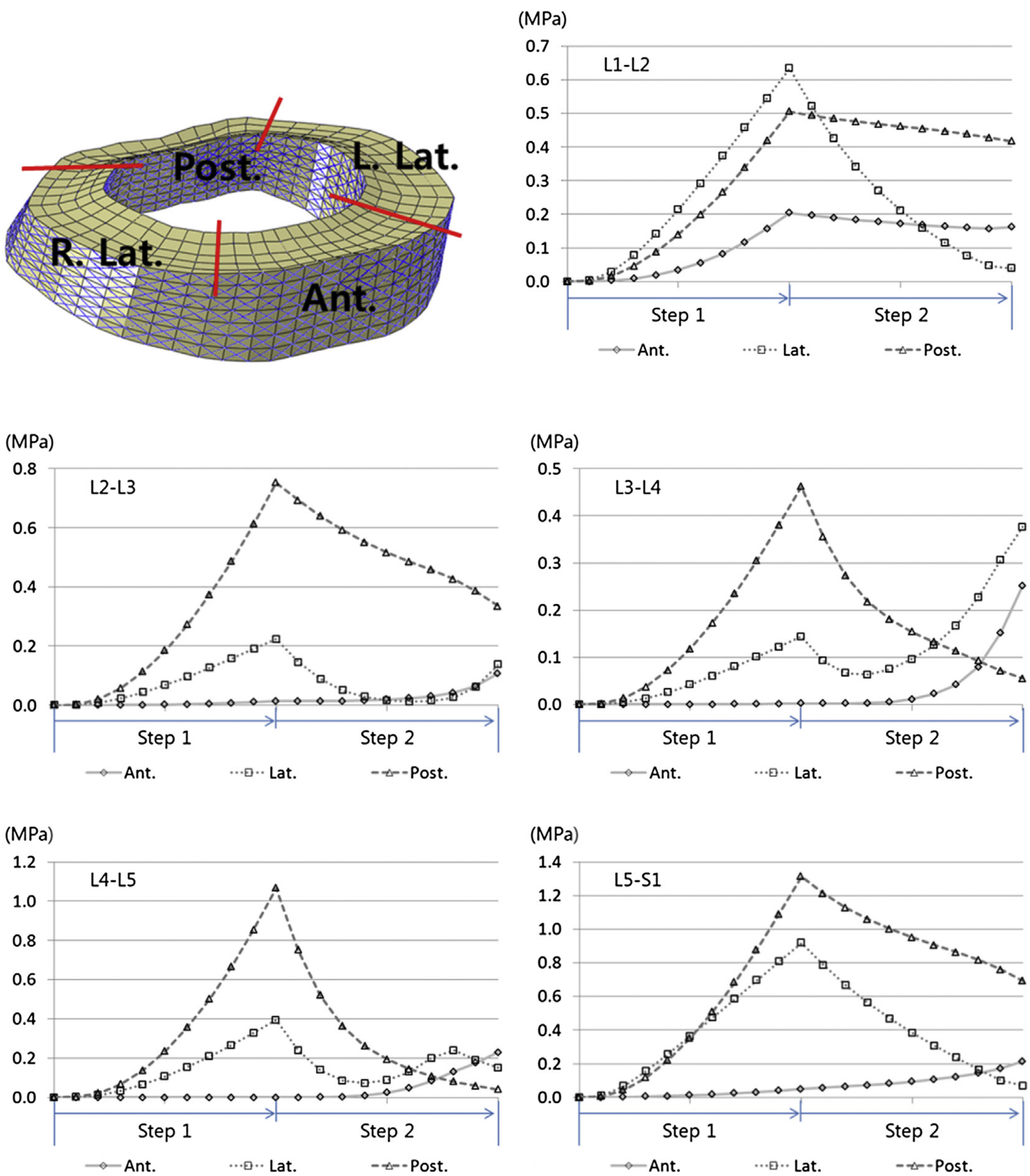

Fig. 4. Average stresses on the fibers of the annulus fibrosus in the anterior (Ant.), lateral (Lat.), and posterior (Post.) regions during two-step traction.

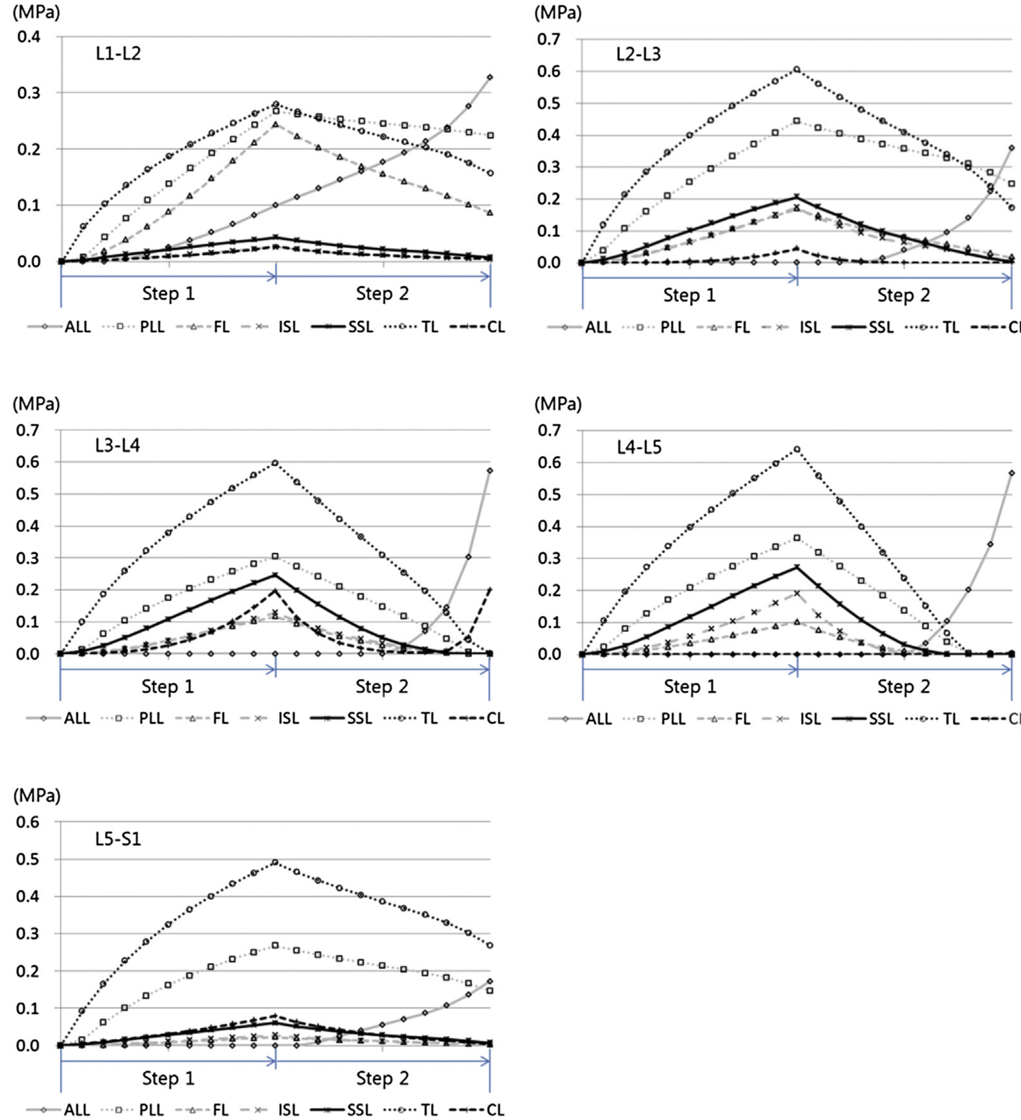

Fig. 5. Stresses on the anterior longitudinal ligament (ALL), posterior longitudinal ligament (PLL), ligamentum flavum (LF), interspinous ligament (ISL), supraspinous ligament (SSL), intertransverse ligament (TL), and capsular ligament (CL) in each motion segment during two-step traction therapy.

the second step of local decompression. While the ALLs in the L2–L3, L3–L4, L4–L5, and L5–S1 MSUs were not stressed during early translation of the L4 vertebra, these ligaments were stressed due to L4 translation of 2.8 mm, 4.2 mm, 4.2 mm, and 1.4 mm, respectively. The stress on the CL at the L3–L4 MSU decreased until the L4 vertebra was translated 4.9 mm in the anterior direction; the stress increased again when the L4 vertebra was translated further. Stresses on the other ligaments decreased with translation of the L4 vertebra.

3.5. Facet joint forces

The facet joint force at the L4–L5 MSU did not occur during the first global axial traction due to joint gap opening. However, this force was generated after 5.6 mm translation of the L4 vertebra during local decompression. When the L4 vertebra was translated as much as 7.0 mm, the force was 36 N. Facet joint forces at the other MSUs did not occur during two-step traction.

4. Discussion

The biomechanical effects of two-step traction on the lumbar spine were investigated. During global axial traction, the intradiscal pressures at all MSUs decreased. At the same time, the lordosis angles at all MSUs decreased, and this resulted in increased stress on the fibers of the annulus fibrosus in the posterior region. The stress on the fibers of the annulus fibrosus in the posterior region was higher for the L4–L5 and L5–S1 MSUs than for the other MSUs. The maximum average stress on the fibers of the annulus fibrosus during global axial traction was 1.1 MPa at L4–L5 MSU and 1.3 MPa at L5–S1 MSU, respectively, which is about 13% and 15% of failure stress of outer posterior annulus (Green et al., 1993). Deen et al. (2003) described a case of disc protrusion in the posterior direction at the L5–S1 MSU during axial traction therapy with VAX-D. The results of the current study may explain why this protrusion occurred. When the annulus fibrosus is weakened by degeneration and/or herniation, it could be damaged more easily by stress concentration, especially at the L5–S1 MSU. Thus, axial traction therapy should be used with caution in patients with intervertebral disc damage at the L4–L5 and/or L5–S1 MSUs.

In this study, the lordosis angle between the superior plane of the L1 vertebra and the superior plane of the sacrum was 44.6° at baseline, 35.2° with global axial traction, and 46.4° with local decompression. This suggests a decrease in the stress on the fibers of the annulus fibrosus in the posterior region of the intervertebral discs by 17–96% during local decompression. However, excessive local decompression resulted in increase of stress on the fibers of the annulus fibrosus in the anterior and lateral regions at the L2–L3, L3–L4, and L4–L5 MSUs. While intradiscal pressure at the L1–L2, L4–L5, and L5–S1 MSUs continuously decreased by 15–45% as translation of the L4 vertebra increased during local decompression, the intradiscal pressure at the L2–L3 and L3–L4 MSUs initially decreased and then increased. Previously published experimental studies have shown that extension motion increases intradiscal pressure at the intervertebral discs (Sato et al., 1999; Rohlmann et al., 2001). Thus, proper local decompression helps decrease the risk of intervertebral disc damage and increases the beneficial effects of reduced intradiscal pressure.

Global axial traction and local decompression resulted in stress on the major ligaments and forces on the facet joints. While the TL and PLL experienced stress primarily during global axial traction, these stresses decreased during local decompression. Iida et al. (2002) reported the average failure strength of ISL and SSL, where it was about 2.6 MPa for the young specimen, and it decreased with aging to about 0.8 MPa for 80 year-old specimen. Even though, failure strength of each ligament of the lumbar spine is not well known, the experienced maximum stress of 0.6 MPa on TL would be high for the elderly persons. Thus, single global traction would have risk of damage at ligaments. Facet joint forces did not arise in any MSUs during global axial traction because axial displacement and the reduction in the lordosis angle of the lumbar spine resulted in axial traction force. However, force at the L4–L5 MSU was generated when the L4 vertebra was translated as much as 5.6 mm; this force was 36 N when the L4 vertebra was translated by 7.0 mm. Thus, excessive local decompression appears to increase the risk of damage in the ligaments and facet joints.

Typically, up to half of a patient's body weight has been used for the axial traction force in manual therapy (Lee and Evans, 2001). However, different traction devices and physical therapists have used different values for axial traction (Macario and Pergolizzi, 2006). For example, Meszaros et al. (2000) reported that 30% and 60% of BW traction is more effective than 10% of BW in traction therapy. In the case report of Deen et al. (2003), axial forces of 334 N were used for traction and 89 N for resting. In the in-vivo experimental study by Ramos and Martin (1994), axial traction forces from 223 N to 445 N were used. No studies have documented the force transmitted through the vertebrae, intervertebral discs, and ligaments, and the translation of the vertebrae during local decompression is also unknown. Thus, 1/3 BW was assumed for global axial traction in this study. Zero to 20% of the anterior–posterior width of the vertebral body in 10% increments was used to generate local decompression.

This study has some limitations and assumptions. First, the model used in this study validated on the aspects of spinal motions. Although stresses on fibers of annulus fibrosus and ligaments were not validated, the results of this study provided relevant results about changes of stresses during two-step traction therapy. Second, with the exception of the intervertebral discs, ligaments, and articular cartilage, all soft-tissues were neglected. Thus, the traction forces were directly transmitted through the vertebrae, ligaments, and intervertebral discs without muscles or skin. This simplification resulted in a greater decrease (0.13 MPa) in intradiscal pressure at L4–L5 during global traction than that (0.03 MPa) was found in the in-vivo study of Ramos and Martin (1994). Third, the initial intradiscal pressure was set to zero in this study; thus, the values for intradiscal pressure are only meaningful as relative values. Fourth, the results of this study were obtained in ideal case of traction therapy for a subject. Thus, to obtain more meaningful results with considering difference of subjects, statistical analyses with considering various subjects would be necessary. Finally, traction therapy consists of elastic and creeping phases due to the viscoelastic material properties of the human body. However, the model used in this study neglected viscosity, and only the elastic phase during two-step traction therapy was analyzed. Despite these limitations and assumptions, the results of this study describe changes in lumbar spine biomechanics during two-step traction therapy.

This study used FE analysis to investigate the biomechanical effects of two-step traction therapy, which consists of global axial traction and local decompression, on the lumbar spine. We found that local decompression was very useful for reducing tensile stress on the fibers of the annulus fibrosus and ligaments generated by the axial traction force for reduction of intradiscal pressure. However, excessive local decompression could result in an increase in intradiscal pressure at the L2–L3 and L3–L4 MSUs, stress on the fibers of the annulus fibrosus in the anterior and lateral regions, stress on the ALL, and facet joint forces. The results of this study could be used to enhance the efficacy of traction therapy and to develop a safer and more effective type of traction therapy that uses a combination of global axial traction and local decompression.

Acknowledgment

This work was supported by 2013 National Agenda Project (NAP) funded by Korea Research Council of Fundamental Science & Technology (NAP-09-2/P-13-JC-LU01-C01). The authors would like to thank Mr. Jae Lak Yang at HANMED CO., LTD for providing information about spinal traction therapy.

References

Apfel CC, Cakmakkaya OS, Martin W, Richmond C, Macario A, George E, et al. Restoration of disk height through non-surgical spinal decompression is associated with decreased discogenic low back pain: a retrospective cohort study. BMC Musculoskelet Disord 2010;11:155.

Daniel DM. Non-surgical spinal decompression therapy: does the scientific literature support efficacy claims made in the advertising media? Chiropr Osteopat 2007;15:7.

Deen Jr HG, Rizzo TD, Fenton DS. Sudden progression of lumbar disk protrusion during vertebral axial decompression traction therapy. Mayo Clin Proc 2003;78:1554–6.

Diab AA, Moustafa IM. Lumbar lordosis rehabilitation for pain and lumbar segmental motion in chronic mechanical low back pain: a randomized trial. J Manipulative Physiol Ther 2012;35:246–53.

Eberlein R, Holzapfel GA, Frohlich M. Multi-segment FEA of the human lumbar spine including the heterogeneity of the annulus fibrosus. Comput Mech 2004;34:147–63.

Gagne AR, Hasson SM. Lumbar extension exercises in conjunction with mechanical traction for the management of a patient with a lumbar herniated disc. Physiother Theor Pract 2010;26:256–66.

Gluck GS, Bendo JA, Spivak JM. The lumbar spine and low back pain in golf: a literature review of swing biomechanics and injury prevention. Spine J 2008;8:778–88.

Goel VK, Monroe BT, Gilbertson LG, Brinckmann P. Interlaminar shear stresses and laminae separation in a disc. Finite element analysis of the L3-L4 motion segment subjected to axial compressive loads. Spine (Phila Pa 1976) 1995;20:689–98.

Green TP, Adams MA, Dolan P. Tensile properties of the annulus fibrosus II. Ultimate tensile strength and fatigue life. Eur Spine J 1993;2:209–14.

Guan Y, Yoganandan N, Zhang J, Pintar FA, Cusick JF, Wolfla CE, et al. Validation of a clinical finite element model of the human lumbosacral spine. Med Biol Eng Comput 2006;44:633–41.

Guan Y, Yoganandan N, Moore J, Pintar FA, Zhang J, Maiman DJ, et al. Moment-rotation responses of the human lumbosacral spinal column. J Biomech 2007;40:1975–80.

ARTICLE IN PRESS

Harrison DE, Cailliet R, Harrison DD, Janik TJ, Holland B. Changes in sagittal lumbar configuration with a new method of extension traction: nonrandomized clinical controlled trial. Arch Phys Med Rehabil 2002a;83:1585–91.
Harrison DE, Cailliet R, Harrison DD, Janik TJ, Holland B. A new 3-point bending traction method for restoring cervical lordosis and cervical manipulation: a nonrandomized clinical controlled trial. Arch Phys Med Rehabil 2002b;83:447–53.
Hilibrand AS, Rand N. Degenerative lumbar stenosis: diagnosis and management. J Am Acad Orthop Surg 1999;7:239–49.
Horseman I, Morningstar MW. Radiographic disk height increase after a trial of multimodal spine rehabilitation and vibration traction: a retrospective case series. J Chiropr Med 2008;7:140–5.
Iida T, Abumi K, Kotani Y, Kaneda K. Effects of aging and spinal degeneration on mechanical properties of lumbar supraspinous and interspinous ligaments. Spine J 2002;2:95–100.
Kelsey JL, White 3rd AA. Epidemiology and impact of low-back pain. Spine (Phila Pa 1976) 1980;5:133–42.
Kim K, Park WM, Kim YH, Lee S. Stress analysis in a pedicle screw fixation system with flexible rods in the lumbar spine. Proc Inst Mech Eng H 2010;224:477–85.
Kurutz M, Bender T. Weightbath hydrotraction treatment: application, biomechanics, and clinical effects. J Multidisciplinary Healthcare 2010;3:19–27.
Kurutz M, Oroszvary L. Finite element analysis of weightbath hydrotraction treatment of degenerated lumbar spine segments in elastic phase. J Biomech 2010;43:433–41.
Lee RY, Evans JH. Loads in the lumbar spine during traction therapy. Aust J Physiother 2001;47:102–8.
Lu YM, Hutton WC, Gharpuray VM. Do bending, twisting, and diurnal fluid changes in the disc affect the propensity to prolapse? A viscoelastic finite element model. Spine (Phila Pa 1976) 1996;21:2570–9.
Macario A, Pergolizzi JV. Systematic literature review of spinal decompression via motorized traction for chronic discogenic low back pain. Pain Pract 2006;6:171–8.
Maher CG. Effective physical treatment for chronic low back pain. Orthop Clin North Am 2004;35:57–64.
Majid K, Fischgrund JS. Degenerative lumbar spondylolisthesis: trends in management. J Am Acad Orthop Surg 2008;16:208–15.
Manchikanti L. Epidemiology of low back pain. Pain Physician 2000;3:167–92.
Meszaros TF, Olson R, Kulig K, Creighton D, Czarnecki E. Effect of 10%, 30%, and 60% body weight traction on the straight leg raise test of symptomatic patients with low back pain. J Orthop Sports Phys Ther 2000;30:595–601.
Moramarco V, Perez del Palomar A, Pappalettere C, Doblare M. An accurate validation of a computational model of a human lumbosacral segment. J Biomech 2010;43:334–42.
Natarajan RN, Andersson GB. The influence of lumbar disc height and cross-sectional area on the mechanical response of the disc to physiologic loading. Spine (Phila Pa 1976) 1999;24:1873–81.
Natarajan RN, Chen BH, An HS, Andersson GB. Anterior cervical fusion: a finite element model study on motion segment stability including the effect of osteoporosis. Spine (Phila Pa 1976) 2000;25:955–61.
Park WM, Kim K, Kim YH. Effects of degenerated intervertebral discs on intersegmental rotations, intradiscal pressures, and facet joint forces of the whole lumbar spine. Comput Biology Med 2013;43:1234–40.
Park WM, Park YS, Kim K, Kim YH. Biomechanical comparison of instrumentation techniques in treatment of thoracolumbar burst fractures: a finite element analysis. J Orthop Sci 2009;14:443–9.
Paulk GP, Harrison DE. Management of a chronic lumbar disk herniation with chiropractic biophysics methods after failed chiropractic manipulative intervention. J Manipulative Physiol Ther 2004;27:579.
Ramos G, Martin W. Effects of vertebral axial decompression on intradiscal pressure. J Neurosurg 1994;81:350–3.
Rohlmann A, Neller S, Bergmann G, Graichen F, Claes L, Wilke HJ. Effect of an internal fixator and a bone graft on intersegmental spinal motion and intradiscal pressure in the adjacent regions. Eur Spine J 2001;10:301–8.
Rohlmann A, Zander T, Schmidt H, Wilke HJ, Bergmann G. Analysis of the influence of disc degeneration on the mechanical behaviour of a lumbar motion segment using the finite element method. J Biomech 2006;39:2484–90.
Ruberte LM, Natarajan RN, Andersson GB. Influence of single-level lumbar degenerative disc disease on the behavior of the adjacent segments—a finite element model study. J Biomech 2009;42:341–8.
Sato K, Kikuchi S, Yonezawa T. In vivo intradiscal pressure measurement in healthy individuals and in patients with ongoing back problems. Spine (Phila Pa 1976) 1999;24:2468–74.
Schmidt H, Heuer F, Simon U, Kettler A, Rohlmann A, Claes L, et al. Application of a new calibration method for a three-dimensional finite element model of a human lumbar annulus fibrosus. Clin Biomech (Bristol, Avon) 2006;21:337–44.
Schmidt H, Kettler A, Heuer F, Simon U, Claes L, Wilke HJ. Intradiscal pressure, shear strain, and fiber strain in the intervertebral disc under combined loading. Spine (Phila Pa 1976) 2007a;32:748–55.
Schmidt H, Kettler A, Rohlmann A, Claes L, Wilke HJ. The risk of disc prolapses with complex loading in different degrees of disc degeneration – a finite element analysis. Clin Biomech (Bristol, Avon) 2007b;22:988–98.
Schmidt H, Heuer F, Wilke HJ. Dependency of disc degeneration on shear and tensile strains between annular fiber layers for complex loads. Med Eng Phys 2009;31:642–9.
Shirazi-Adl A, Ahmed AM, Shrivastava SC. Mechanical response of a lumbar motion segment in axial torque alone and combined with compression. Spine (Phila Pa 1976) 1986;11:914–27.
Ueno K, Liu YK. A three-dimensional nonlinear finite element model of lumbar intervertebral joint in torsion. J Biomech Eng 1987;109:200–9.
Wagner DR, Lotz JC. Theoretical model and experimental results for the nonlinear elastic behavior of human annulus fibrosus. J Orthop Res 2004;22:901–9.
Zander T, Rohlmann A, Calisse J, Bergmann G. Estimation of muscle forces in the lumbar spine during upper-body inclination. Clin Biomech (Bristol, Avon) 2001;16(Suppl. 1):S73–80.

Please cite this article in press as: Park WM, et al., Biomechanical analysis of two-step traction therapy in the lumbar spine, Manual Therapy (2014), http://dx.doi.org/10.1016/j.math.2014.05.004